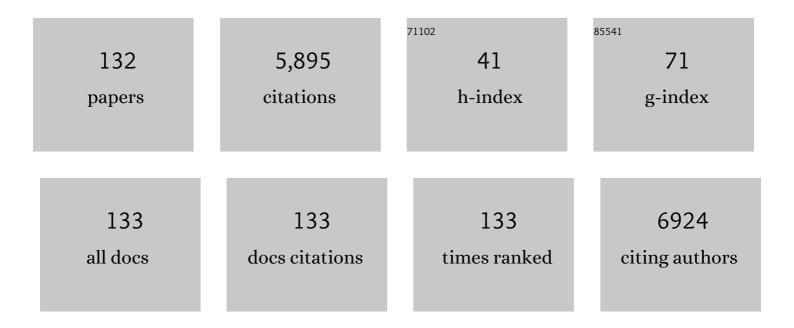
## **Xiang-Fang Peng**

List of Publications by Year in descending order

Source: https://exaly.com/author-pdf/8502461/publications.pdf Version: 2024-02-01



#	Article	IF	CITATIONS
1	A facile structural manipulation strategy to prepare ultra-strong, super-tough, and thermally stable polylactide/nucleating agent composites. Advanced Composites and Hybrid Materials, 2022, 5, 948-959.	21.1	46
2	External flow-induced highly oriented and dense nanohybrid shish-kebabs: A strategy for achieving high performance in poly (lactic acid) composites. Composites Communications, 2022, 29, 101042.	6.3	26
3	Supercritical Fluids-Assisted Processing Using CO2 Foaming to Enhance the Dispersion of Nanofillers in Poly(butylene succinate)-Based Nanocomposites and the Conductivity. Journal of Polymers and the Environment, 2022, 30, 3063-3077.	5.0	4
4	Solar-assisted high-efficient cleanup of viscous crude oil spill using an ink-modified plant fiber sponge. Journal of Hazardous Materials, 2022, 432, 128740.	12.4	23
5	Highly strong and sensitive bilayer hydrogel actuators enhanced by cross-oriented nanocellulose networks. Composites Science and Technology, 2022, 225, 109494.	7.8	16
6	Photochromic properties of ruthenium complexes with dithienylethene-ethynylthiophene. Dyes and Pigments, 2021, 184, 108750.	3.7	3
7	Exceptional size-dependent property of TiS2 nanosheets for optical limiting. Applied Surface Science, 2021, 541, 148371.	6.1	21
8	Synergistic enhancement of thermal conductivity by addition of graphene nanoplatelets to threeâ€dimensional boron nitride scaffolds for polyamide 6 composites. Polymer Engineering and Science, 2021, 61, 1415-1426.	3.1	11
9	Highly Strong and Conductive Carbon Fibers Originated from Bioinspired Lignin/Nanocellulose Precursors Obtained by Flow-Assisted Alignment and In Situ Interfacial Complexation. ACS Sustainable Chemistry and Engineering, 2021, 9, 2591-2599.	6.7	24
10	The effect of polytetrafluoroethylene particle size on the properties of biodegradable poly(butylene) Tj ETQq0 0 (	) rgBT /Ov	erlock 10 Tf
11	Superior mechanical performance of in-situ nanofibrillar HDPE/PTFE composites with highly oriented and compacted nanohybrid shish-kebab structure. Composites Science and Technology, 2021, 207, 108715.	7.8	17
12	Muscle-inspired double-network hydrogels with robust mechanical property, biocompatibility and ionic conductivity. Carbohydrate Polymers, 2021, 262, 117936.	10.2	43

13	Highly Stretchable, Self-Healable, Freezing-Tolerant, and Transparent Polyacrylic Acid/Nanochitin Composite Hydrogel for Self-Powered Multifunctional Sensors. ACS Sustainable Chemistry and Engineering, 2021, 9, 9209-9220.	6.7	76
14	Interfacial polyelectrolyte complexation spinning of graphene/cellulose nanofibrils for fiber-shaped electrodes. Journal of Materials Research, 2020, 35, 122-131.	2.6	8
15	Dual super-amphiphilic modified cellulose acetate nanofiber membranes with highly efficient oil/water separation and excellent antifouling properties. Journal of Hazardous Materials, 2020, 385, 121582.	12.4	96
16	Fabrication of bimodal open-porous poly (butylene succinate)/cellulose nanocrystals composite scaffolds for tissue engineering application. International Journal of Biological Macromolecules, 2020, 147, 1164-1173.	7.5	52
17	Fabrication of Poly(lactic acid)/Silkworm Excrement Composite with Enhanced Crystallization, Toughness and Biodegradation Properties. Journal of Polymers and the Environment, 2020, 28, 295-303.	5.0	6

 Facile fabrication of fully biodegradable and biorenewable poly (lactic acid)/poly (butylene) Tj ETQq0 0 0 rgBT /Overlock 10 Tf 50 67 Td (

 18
 5.8
 33

excellent heat resistance. Polymer Degradation and Stability, 2020, 171, 109044.

#	Article	IF	CITATIONS
19	Fibrous form-stable phase change materials with high thermal conductivity fabricated by interfacial polyelectrolyte complex spinning. Carbohydrate Polymers, 2020, 249, 116836.	10.2	30
20	Hierarchical Assembly of Nanocellulose into Filaments by Flow-Assisted Alignment and Interfacial Complexation: Conquering the Conflicts between Strength and Toughness. ACS Applied Materials & Interfaces, 2020, 12, 32090-32098.	8.0	29
21	Lightweight multifunctional polypropylene/carbon nanotubes/carbon black nanocomposite foams with segregated structure, ultralow percolation threshold and enhanced electromagnetic interference shielding performance. Composites Science and Technology, 2020, 193, 108116.	7.8	110
22	Highly Efficient Removal of Methylene Blue Dye from an Aqueous Solution Using Cellulose Acetate Nanofibrous Membranes Modified by Polydopamine. ACS Omega, 2020, 5, 5389-5400.	3.5	170
23	Microwaveâ€assisted in situ polymerization of polycaprolactone/boron nitride composites with enhanced thermal conductivity and mechanical properties. Polymer International, 2020, 69, 635-643.	3.1	9
24	Study on the mechanical and thermal properties of polylactic acid/hydroxyapatite@polydopamine composite nanofibers for tissue engineering. Journal of Applied Polymer Science, 2020, 137, 49077.	2.6	13
25	Synergetic effect of nanoclay and nano-CaCO <sub>3</sub> hybrid filler systems on the foaming properties and cellular structure of polystyrene nanocomposite foams using supercritical CO <sub>2</sub> . Frontiers in Forests and Global Change, 2020, 39, 185-202.	1.1	5
26	<i>In situ</i> Polymerization of Polyamide 6/Boron Nitride Composites to Enhance Thermal Conductivity and Mechanical Properties <i>via</i> Boron Nitride Covalently Grafted Polyamide 6. Polymer Engineering and Science, 2020, 60, 710-716.	3.1	16
27	Reflux pretreatment-mediated sonication: A new universal route to obtain 2D quantum dots. Materials Today, 2019, 22, 17-24.	14.2	12
28	Preparation of fastâ€degrading poly(lactic acid)/soy protein concentrate biocomposite foams via supercritical CO <sub>2</sub> foaming. Polymer Engineering and Science, 2019, 59, 1753-1762.	3.1	13
29	Effect of dynamic oscillation shear flow intensity on the mechanical and morphological properties of high-density polyethylene: An integrated experimental and molecular dynamics simulation study. Polymer Testing, 2019, 80, 106122.	4.8	11
30	An improved technique for dispersion of natural graphite particles in thermoplastic polyurethane by sub-critical gas-assisted processing. Composites Science and Technology, 2019, 182, 107783.	7.8	20
31	Highly Durable Superhydrophobic Polymer Foams Fabricated by Extrusion and Supercritical CO <sub>2</sub> Foaming for Selective Oil Absorption. ACS Applied Materials & Interfaces, 2019, 11, 7479-7487.	8.0	72
32	Nitrogen-doped carbon-coated Fe3O4/rGO nanocomposite anode material for enhanced initial coulombic efficiency of lithium-ion batteries. Ionics, 2019, 25, 1513-1521.	2.4	11
33	Isotope Effects on the Crystallization Kinetics of Selectively Deuterated Poly(ε aprolactone). Journal of Polymer Science, Part B: Polymer Physics, 2019, 57, 771-779.	2.1	9
34	High performance high-density polyethylene/hydroxyapatite nanocomposites for load-bearing bone substitute: fabrication, in vitro and in vivo biocompatibility evaluation. Composites Science and Technology, 2019, 175, 100-110.	7.8	50
35	Fabrication of Poly(butylene succinate) phosphorus-containing ionomers microcellular foams with significantly improved thermal conductivity and compressive strength. Polymer, 2019, 185, 121967.	3.8	28
36	High-performance porous PLLA-based scaffolds for bone tissue engineering: Preparation, characterization, and in vitro and in vivo evaluation. Polymer, 2019, 180, 121707.	3.8	81

#	Article	IF	CITATIONS
37	Using H2O2 to selectively oxidize recyclable cellulose yarn with high carboxyl content. Cellulose, 2019, 26, 2699-2713.	4.9	22
38	A facile approach towards fabrication of lightweight biodegradable poly (butylene succinate)/carbon fiber composite foams with high electrical conductivity and strength. Composites Science and Technology, 2018, 159, 171-179.	7.8	74
39	In-situ fibrillated polytetrafluoroethylene (PTFE) in thermoplastic polyurethane (TPU) via melt blending: Effect on rheological behavior, mechanical properties, and microcellular foamability. Polymer, 2018, 134, 263-274.	3.8	98
40	Synthesis of DOPO-HQ-functionalized graphene oxide as a novel and efficient flame retardant and its application on polylactic acid: Thermal property, flame retardancy, and mechanical performance. Journal of Colloid and Interface Science, 2018, 524, 267-278.	9.4	99
41	Polylactide/thermoplastic polyurethane/polytetrafluoroethylene nanocomposites with in situ fibrillated polytetrafluoroethylene and nanomechanical properties at the interface using atomic force microscopy. Polymer Testing, 2018, 67, 22-30.	4.8	23
42	Understanding the Mechanistic Behavior of Highly Charged Cellulose Nanofibers in Aqueous Systems. Macromolecules, 2018, 51, 1498-1506.	4.8	92
43	Polyamide 6 modified polypropylene with remarkably enhanced mechanical performance, thermal properties, and foaming ability <i>via</i> pressureâ€inducedâ€flow processing approach. Advances in Polymer Technology, 2018, 37, 2721-2729.	1.7	18
44	Fabrication and mechanism of poly(butylene succinate) urethane ionomer microcellular foams with high thermal insulation and compressive feature. European Polymer Journal, 2018, 99, 250-258.	5.4	47
45	Superhydrophobic Graphene/Cellulose/Silica Aerogel with Hierarchical Structure as Superabsorbers for High Efficiency Selective Oil Absorption and Recovery. Industrial & Engineering Chemistry Research, 2018, 57, 1745-1755.	3.7	69
46	Fabricationâ€controlled morphology of poly(butylene succinate) nanoâ€microcellular foams by supercritical <scp>CO</scp> <sub>2</sub> . Polymers for Advanced Technologies, 2018, 29, 1953-1965.	3.2	9
47	Formation of stretched fibrils and nanohybrid shish-kebabs in isotactic polypropylene-based nanocomposites by application of a dynamic oscillatory shear. Chemical Engineering Journal, 2018, 348, 546-556.	12.7	33
48	Hybrids of aluminum hypophosphite and ammonium polyphosphate: Highly effective flame retardant system for unsaturated polyester resin. Polymer Composites, 2018, 39, 1763-1770.	4.6	26
49	A new two-step process to prepare microcellular epoxy foams based on kinetic analysis. Journal of Materials Science, 2018, 53, 1540-1555.	3.7	9
50	Phosphorylated chitosanâ€cobalt complex: A novel green flame retardant for polylactic acid. Polymers for Advanced Technologies, 2018, 29, 860-866.	3.2	31
51	Electrospun poly (butylene succinate)/cellulose nanocrystals bio-nanocomposite scaffolds for tissue engineering: Preparation, characterization and in vitro evaluation. Polymer Testing, 2018, 71, 101-109.	4.8	79
52	Electrospinning and crosslinking of polyvinyl alcohol/chitosan composite nanofiber for transdermal drug delivery. Advances in Polymer Technology, 2018, 37, 1917-1928.	1.7	148
53	Ultra-strong, tough and high wear resistance high-density polyethylene for structural engineering application: A facile strategy towards using the combination of extensional dynamic oscillatory shear flow and ultra-high-molecular-weight polyethylene. Composites Science and Technology, 2018, 167, 301-312.	7.8	29
54	Highly Stretchable and Biocompatible Strain Sensors Based on Mussel-Inspired Super-Adhesive Self-Healing Hydrogels for Human Motion Monitoring. ACS Applied Materials & Interfaces, 2018, 10, 20897-20909.	8.0	398

#	Article	IF	CITATIONS
55	Structural evolution of uniaxial tensile-deformed injection molded poly(É›-caprolactone)/hydroxyapatite composites. Polymer Composites, 2017, 38, 1771-1782.	4.6	4
56	Poly (propylene carbonate)-based in situ nanofibrillar biocomposites with enhanced miscibility, dynamic mechanical properties, rheological behavior and extrusion foaming ability. Composites Part B: Engineering, 2017, 123, 112-123.	12.0	62
57	Superior Impact Toughness and Excellent Storage Modulus of Poly(lactic acid) Foams Reinforced by Shish-Kebab Nanoporous Structure. ACS Applied Materials & Interfaces, 2017, 9, 21071-21076.	8.0	69
58	Rheological Properties of Jute-Based Cellulose Nanofibers under Different Ionic Conditions. ACS Symposium Series, 2017, , 113-132.	0.5	8
59	Structure characterization of cellulose nanofiber hydrogel as functions of concentration and ionic strength. Cellulose, 2017, 24, 5417-5429.	4.9	59
60	Magnetic Nanocarbon Adsorbents with Enhanced Hexavalent Chromium Removal: Morphology Dependence of Fibrillar vs Particulate Structures. Industrial & Engineering Chemistry Research, 2017, 56, 10689-10701.	3.7	267
61	Surface Modification of Electrospun TPU Nanofiber Scaffold with CNF Particles by Ultrasoundâ€Assisted Technique for Tissue Engineering. Macromolecular Materials and Engineering, 2017, 302, 1700277.	3.6	20
62	Fabrication of poly(ε-caprolactone) tissue engineering scaffolds with fibrillated and interconnected pores utilizing microcellular injection molding and polymer leaching. RSC Advances, 2017, 7, 43432-43444.	3.6	75
63	Mechanical properties, crystallization characteristics, and foaming behavior of polytetrafluoroethylene-reinforced poly(lactic acid) composites. Polymer Engineering and Science, 2017, 57, 570-580.	3.1	44
64	Improved crystallizability and processability of ultra high molecular weight polyethylene modified by poly(amido amine) dendrimers. Polymer Engineering and Science, 2017, 57, 153-160.	3.1	15
65	Molecular Beacon Nano-Sensors for Probing Living Cancer Cells. Trends in Biotechnology, 2017, 35, 347-359.	9.3	58
66	Facile preparation of open-cellular porous poly (l-lactic acid) scaffold by supercritical carbon dioxide foaming for potential tissue engineering applications. Chemical Engineering Journal, 2017, 307, 1017-1025.	12.7	193
67	Cell evolution and compressive properties of styrene–butadiene–styrene toughened and calcium carbonate reinforced polystyrene extrusion foams with supercritical carbon dioxide. Journal of Applied Polymer Science, 2016, 133, .	2.6	17
68	Comparatively Thermal and Crystalline Study of Poly(methylâ€methacrylate)/Polyacrylonitrile Hybrids: Core–Shell Hollow Fibers, Porous Fibers, and Thin Films. Macromolecular Materials and Engineering, 2016, 301, 1327-1336.	3.6	22
69	Matrigel immobilization on the shish-kebab structured poly(ε-caprolactone) nanofibers for skin tissue engineering. AIP Conference Proceedings, 2016, , .	0.4	3
70	Enhanced strength and foamability of high-density polyethylene prepared by pressure-induced flow and low-temperature crosslinking. RSC Advances, 2016, 6, 34422-34427.	3.6	18
71	Formation of nanoscale pores in shish-kebab structured isotactic polypropylene by supercritical CO2 foaming. Materials Letters, 2016, 167, 274-277.	2.6	20
72	Facile preparation of lightweight high-strength biodegradable polymer/multi-walled carbon nanotubes nanocomposite foams for electromagnetic interference shielding. Carbon, 2016, 105, 305-313.	10.3	374

#	Article	IF	CITATIONS
73	The Effect of Talc on the Mechanical, Crystallization and Foaming Properties of Poly(Lactic Acid). Journal of Macromolecular Science - Physics, 2016, 55, 908-924.	1.0	13
74	Synthesis of a novel highly effective flame retardant containing multivalent phosphorus and its application in unsaturated polyester resins. RSC Advances, 2016, 6, 86632-86639.	3.6	35
75	Investigation of poly( <scp> </scp> -lactic acid)/graphene oxide composites crystallization and nanopore foaming behaviors via supercritical carbon dioxide low temperature foaming. Journal of Materials Research, 2016, 31, 348-359.	2.6	22
76	Preparation of highly porous interconnected poly(lactic acid) scaffolds based on a novel dynamic elongational flow procedure. Materials and Design, 2016, 101, 285-293.	7.0	25
77	Fabrication of polystyrene/nanoâ€ <scp>C</scp> a <scp>CO</scp> <sub>3</sub> foams with unimodal or bimodal cell structure from extrusion foaming using supercritical carbon dioxide. Polymer Composites, 2016, 37, 1864-1873.	4.6	9
78	Excellent properties and extrusion foaming behavior of PPC/PS/PTFE composites with an in situ fibrillated PTFE nanofibrillar network. RSC Advances, 2016, 6, 3176-3185.	3.6	19
79	Supercritical CO2 foaming of pressure-induced-flow processed linear polypropylene. Materials and Design, 2016, 93, 509-513.	7.0	43
80	Complex cellular structure evolution of polystyrene/poly (ethylene terephthalate glycol-modified) foam using a two-step depressurization batch foaming process. Journal of Cellular Plastics, 2016, 52, 595-618.	2.4	12
81	In vitro evaluations of electrospun nanofiber scaffolds composed of poly(É>-caprolactone) and polyethylenimine. Journal of Materials Research, 2015, 30, 1808-1819.	2.6	23
82	Magnetic epoxy nanocomposites with superparamagnetic MnFe2O4 nanoparticles. AIP Advances, 2015, 5,	1.3	12
83	Novel foaming method to fabricate microcellular injection molded polycarbonate parts using sodium chloride and active carbon as nucleating agents. Polymer Engineering and Science, 2015, 55, 1634-1642.	3.1	12
84	Effect of Poly(butylenes succinate) on Poly(lactic acid) Foaming Behavior: Formation of Open Cell Structure. Industrial & Engineering Chemistry Research, 2015, 54, 6199-6207.	3.7	84
85	Ultrasound-assisted-pressure-induced-flow leading to superior polymer/carbon nanotube composites and foams. Polymer, 2015, 80, 237-244.	3.8	23
86	Electrospinning thermoplastic polyurethane/graphene oxide scaffolds for small diameter vascular graft applications. Materials Science and Engineering C, 2015, 49, 40-50.	7.3	122
87	Electrospun aligned poly(propylene carbonate) microfibers with chitosan nanofibers as tissue engineering scaffolds. Carbohydrate Polymers, 2015, 117, 941-949.	10.2	76
88	Fabrication of Poly(lactic acid)/Graphene Oxide Foams with Highly Oriented and Elongated Cell Structure via Unidirectional Foaming Using Supercritical Carbon Dioxide. Industrial & Engineering Chemistry Research, 2015, 54, 758-768.	3.7	124
89	Shish-Kebab-Structured Poly(ε-Caprolactone) Nanofibers Hierarchically Decorated with Chitosan–Poly(ε-Caprolactone) Copolymers for Bone Tissue Engineering. ACS Applied Materials & Interfaces, 2015, 7, 6955-6965.	8.0	126
90	A novel multiple soaking temperature (MST) method to prepare polylactic acid foams with bi-modal open-pore structure and their potential in tissue engineering applications. Journal of Supercritical Fluids, 2015, 103, 28-37.	3.2	18

6

#	Article	IF	CITATIONS
91	Enhancing Nanofiller Dispersion Through Prefoaming and Its Effect on the Microstructure of Microcellular Injection Molded Polylactic Acid/Clay Nanocomposites. Industrial & Engineering Chemistry Research, 2015, 54, 7122-7130.	3.7	34
92	Morphology Evolution of the Microcellular Polymethyl Methacrylate with Supercritical CO <sub>2</sub> : Effects of Shear Stress and Orthogonal Vibration. Polymer-Plastics Technology and Engineering, 2015, 54, 822-836.	1.9	2
93	Fabrication of polylactic acid/polyethylene glycol ( <scp>PLA</scp> / <scp>PEG</scp> ) porous scaffold by supercritical <scp>CO</scp> <sub>2</sub> foaming and particle leaching. Polymer Engineering and Science, 2015, 55, 1339-1348.	3.1	48
94	Hierarchically decorated electrospun poly( \$\$ varepsilon \$\$ ε -caprolactone)/nanohydroxyapatite composite nanofibers for bone tissue engineering. Journal of Materials Science, 2015, 50, 4174-4186.	3.7	17
95	The morphology, properties, and shape memory behavior of polylactic acid/thermoplastic polyurethane blends. Polymer Engineering and Science, 2015, 55, 70-80.	3.1	106
96	The Preliminary Study on Polylactide/Polystyrene/Nanoclay Composites. , 2015, , .		0
97	Fabrication of high strength PA6/PP blends with pressure-induced-flow processing. Materials Chemistry and Physics, 2015, 164, 1-5.	4.0	21
98	Preparation of Novel c-6 Position Carboxyl Corn Starch by a Green Method and Its Application in Flame Retardance of Epoxy Resin. Industrial & Engineering Chemistry Research, 2015, 54, 11944-11952.	3.7	36
99	Properties and fibroblast cellular response of soft and hard thermoplastic polyurethane electrospun nanofibrous scaffolds. Journal of Biomedical Materials Research - Part B Applied Biomaterials, 2015, 103, 960-970.	3.4	30
100	Fabrication of thermoplastic polyurethane tissue engineering scaffold by combining microcellular injection molding and particle leaching. Journal of Materials Research, 2014, 29, 911-922.	2.6	42
101	Approach to Fabricating Thermoplastic Polyurethane Blends and Foams with Tunable Properties by Twinâ€Screw Extrusion and Microcellular Injection Molding. Advances in Polymer Technology, 2014, 33,	1.7	19
102	Numerical Simulation of Mixing Characteristics in a Vane Extruder. Journal of Macromolecular Science - Physics, 2014, 53, 358-369.	1.0	4
103	Morphology, mechanical properties, and mineralization of rigid thermoplastic polyurethane/hydroxyapatite scaffolds for bone tissue applications: effects of fabrication approaches and hydroxyapatite size. Journal of Materials Science, 2014, 49, 2324-2337.	3.7	60
104	Simultaneous reinforcing and toughening of high impact polystyrene with a novel processing method of loop oscillating push–pull molding. Materials Letters, 2014, 123, 55-58.	2.6	12
105	Effect of poly(ethylene glycol) on the properties and foaming behavior of macroporous poly(lactic) Tj ETQq1 1 C	).784314 r 2.6	gBT_{Overloc
106	Poly(ε-caprolactone) (PCL)/cellulose nano-crystal (CNC) nanocomposites and foams. Cellulose, 2014, 21, 2727-2741.	4.9	107
107	Preparation of thermoplastic polyurethane/graphene oxide composite scaffolds by thermally induced phase separation. Polymer Composites, 2014, 35, 1408-1417.	4.6	45
108	Electrospinning Homogeneous Nanofibrous Poly(propylene carbonate)/Gelatin Composite Scaffolds for Tissue Engineering. Industrial & Engineering Chemistry Research, 2014, 53, 9391-9400.	3.7	45

#	Article	IF	CITATIONS
109	Morphology, mechanical properties, and shape memory effects of poly(lactic acid)/ thermoplastic polyurethane blend scaffolds prepared by thermally induced phase separation. Journal of Cellular Plastics, 2014, 50, 361-379.	2.4	45
110	A novel thermoplastic polyurethane scaffold fabrication method based on injection foaming with water and supercritical carbon dioxide as coblowing agents. Polymer Engineering and Science, 2014, 54, 2947-2957.	3.1	41
111	Characterization of thermoplastic polyurethane/polylactic acid (TPU/PLA) tissue engineering scaffolds fabricated by microcellular injection molding. Materials Science and Engineering C, 2013, 33, 4767-4776.	7.3	235
112	Characterization and properties of electrospun thermoplastic polyurethane blend fibers: Effect of solution rheological properties on fiber formation. Journal of Materials Research, 2013, 28, 2339-2350.	2.6	40
113	Comparisons of microcellular polylactic acid parts injection molded with supercritical nitrogen and expandable thermoplastic microspheres: Surface roughness, tensile properties, and morphology. Journal of Cellular Plastics, 2013, 49, 33-45.	2.4	11
114	Influence and prediction of processing parameters on the properties of microcellular injection molded thermoplastic polyurethane based on an orthogonal array test. Journal of Cellular Plastics, 2013, 49, 439-458.	2.4	31
115	Processing and characterization of supercritical CO <sub>2</sub> batch foamed poly(lactic) Tj ETQq1 1 0.784314 Science, 2013, 130, 3066-3073.	ł rgBT /Ov 2.6	erlock 10 Tf 47
116	Entrance Length of Polymer Flow Through a Contraction Die: Comparison of Calculation from an Equation and Flow Induced Birefringence Measurements. Journal of Macromolecular Science - Physics, 2012, 51, 946-955.	1.0	0
117	Comparisons of microcellular polylactic acid parts injection molded with supercritical nitrogen and expandable thermoplastic microspheres: Surface roughness, tensile properties, and morphology. Journal of Cellular Plastics, 2012, 48, 433-444.	2.4	7
118	Effect of Stretching on <i>β</i> -Phase Content of Isotactic Polypropylene Melt Containing <i>β</i> -Nucleating Agent. Journal of Macromolecular Science - Physics, 2012, 51, 828-838.	1.0	4
119	Enhanced orientation of the waterâ€assisted injectionâ€molded ipp in the presence of nucleating agent. Polymer Engineering and Science, 2012, 52, 725-732.	3.1	22
120	A new microcellular injection molding process for polycarbonate using water as the physical blowing agent. Polymer Engineering and Science, 2012, 52, 1464-1473.	3.1	25
121	The hierarchical structure of waterâ€assisted injection molded high density polyethylene: Small angle Xâ€ray scattering study. Journal of Applied Polymer Science, 2012, 125, 2297-2303.	2.6	19
122	Transcrystallization in nanofiber bundle/isotactic polypropylene composites: effect of matrix molecular weight. Colloid and Polymer Science, 2012, 290, 1157-1164.	2.1	14
123	HDPE solution crystallization induced by electrospun PA66 nanofiber. Colloid and Polymer Science, 2011, 289, 843-848.	2.1	13
124	Negative effect of stretching on the development of βâ€phase in βâ€nucleated isotactic polypropylene. Polymer International, 2011, 60, 1016-1023.	3.1	9
125	Oriented structure in stretched isotactic polypropylene melt and its unexpected recrystallization: optical and Xâ€ray studies. Polymer International, 2011, 60, 1434-1441.	3.1	17
126	Competing effect of shear and β-nucleating agent on the crystallization of injection-molded iPP. E-Polymers, 2010, 10, .	3.0	0

#	Article	IF	CITATIONS
127	Suppression of β-crystal in iPP/PET Fiber Composites. Polymer-Plastics Technology and Engineering, 2010, 49, 154-157.	1.9	8
128	Reinforcing and toughening on poly(ether imide) by a novel thermo tropic liquid crystalline poly(esterâ€imideâ€ketone) with low content. Polymer Engineering and Science, 2009, 49, 2046-2053.	3.1	3
129	Skin Thickness and β-Crystals Development in Injection-Molded iPP Along the Flow Direction. Journal of Macromolecular Science - Physics, 2009, 48, 439-448.	1.0	3
130	An electromagnetic dynamic film blowing technology for mLLDPE. Journal of Applied Polymer Science, 2006, 101, 83-89.	2.6	5
131	Optimized Polystyrene Cell Morphology by Orthogonal Superposition of Oscillatory Shear. Polymer-Plastics Technology and Engineering, 2006, 45, 1025-1029.	1.9	15
132	Interfacial Polyelectrolyte Complexation Spinning of Cellulose Nanofibers/CdTe Quantum Dots for Anti-counterfeiting Fluorescent Textiles. Fibers and Polymers, 0, , 1.	2.1	1